ELSEVIER

Biophysical Chemistry 83 (2000) 153–170

Biophysical Chemistry

www.elsevier.nl/locate/bpc

Oscillations and bistability predicted by a model for a cyclical bienzymatic system involving the regulated isocitrate dehydrogenase reaction

Gianluca M. Guidi, Albert Goldbeter*

Faculté des Sciences, Université Libre de Bruxelles, Campus Plaine, C.P. 231, B-1050 Brussels, Belgium

Received 12 July 1999; received in revised form 4 November 1999; accepted 4 November 1999

Abstract

We analyze the dynamics of a bienzymatic system consisting of isocitrate dehydrogenase (IDH, EC. 1.1.1.42), which transforms $NADP^+$ into NADPH, and of diaphorase (DIA, EC 1.8.1.4), which catalyzes the reverse reaction. Experimental evidence as well as a theoretical model showed the possibility of a coexistence between two stable steady states in this reaction system [G.M. Guidi et al. Biophys. J. 74 (1998) 1229–1240], owing to the regulatory properties of IDH. Here we extend this analysis by considering the behavior of the model proposed for the IDH–DIA bienzymatic system in conditions where the system is open to an influx of its substrates isocitrate and $NADP^+$ and to an efflux of all metabolic species. The analysis indicates that in addition to different modes of bistability (including mushrooms and isolas), sustained oscillations can be observed in such conditions. These results point to the isocitrate dehydrogenase reaction coupled to diaphorase as a suitable candidate for further experimental and theoretical studies of bistability and oscillations in biochemical systems. The results obtained in this particular bienzymatic system bear on other enzymatic systems possessing a cyclical nature, which are known to play significant roles in a variety of metabolic and cellular regulatory processes.

* Corresponding author. Tel.: +32-2-650-5772; fax: +32-2-650-5767.
E-mail address: agoldbet@ulb.ac.be (A. Goldbeter)

0301-4622/00/$ - see front matter
PII: S0301-4622(99)00136-2

1. Introduction

Sustained oscillations and bistability, i.e. the coexistence between two stable steady states, represent two of the most common modes of dynamic self-organization in regulated biochemical and biological systems. Several experimental examples of oscillations are known in biochemistry, as best illustrated by the peroxidase reaction, glycolytic oscillations in yeast, muscle, and other cell types, and cyclic AMP oscillations in *Dictyostelium* cells (see Goldbeter [1] and Hess [2] for recent reviews of biochemical oscillations). Bistability has also been demonstrated experimentally in a number of biochemical systems, a.o. the peroxidase reaction [3] and a reconstituted glycolytic system [4]. The number of examples in which both oscillations and bistability occur in closely related conditions remains, however, reduced. It is therefore of interest to investigate possible new biochemical reactions capable of giving rise to these two self-organization phenomena. This would allow us to better understand the relationship between the two types of dynamic behavior, and to better delineate the conditions in which they occur.

In a previous article [5] we focused on the occurrence of bistability in the isocitrate dehydrogenase (IDH, EC. 1.1.1.42) reaction which is subjected to a variety of positive and negative feedback regulations exerted by its substrate $NADP^+$ and its product NADPH [6–10]. By means of a theoretical model based on these regulatory properties we accounted for the experimental observations of Carlier [5,10] who showed that bistable behavior can occur in the IDH reaction when the latter is coupled to a second reaction catalyzed by diaphorase (DIA, EC 1.8.1.4) which transforms NADPH back into $NADP^+$. Here we extend the analysis of this model, in order to clarify the conditions in which sustained oscillations might occur in this experimental system.

As a first step we introduce an influx of the substrate isocitrate, and keep the total amount of $NADP^+ + NADPH$ constant, as in the experimental conditions considered by Carlier. We have previously reported preliminary results on the occurrence of sustained oscillations in such semi-open conditions [11]. Here we obtain analytical results, which indicate the region in parameter space where sustained oscillations can then be found. Bistability, however, cannot occur in these conditions. Next we show that both bistability and oscillations can occur in fully open conditions, when the two substrates are supplied at a constant rate and when all metabolic species are allowed to flow out of the system. The results of this theoretical study should help to pinpoint the conditions in which oscillations might be observed experimentally in the IDH–DIA bienzymatic system and bring to light the link between bistability and oscillations.

The analysis of bistability and oscillations in the IDH–diaphorase bienzymatic system is of special interest for metabolic regulation, since there exist many instances in which different enzymes catalyze opposite reactions. In addition, many important physiological processes — including those involving some oncogene products, signal transduction and cell proliferation — are controlled by kinases and phosphatases which are organized in a cyclical manner, like the enzymatic system considered in this paper. Here, however, a key role in bistability and oscillations is played by the regulation of IDH by its reaction product, a peculiarity that is not necessarily shared by other enzymes that are part of such cycles. Understanding the conditions in which bistability or oscillations can occur in cyclically organized enzyme reactions is thus of primary importance, beyond the particular case of the IDH–DIA system which could serve as a good prototype for the study of such phenomena in in vitro conditions.

The interest of focusing on the IDH–DIA coupled reactions is that experimental observations accounted for by our previous analysis have already provided evidence for bistable behavior in this system. The present extension of the model to the case of oscillations and non-transient bistability in open conditions is strengthened by the validation of the previous version which accounted in a qualitative and quantitative manner for observations on transient bistability in closed conditions.

2. Model for the IDH–DIA reactions with input of isocitrate

Bistability was demonstrated experimentally and theoretically in the IDH reaction which transforms $NADP^+$ into NADPH when a second enzyme, diaphorase, was used to transform NADPH into $NADP^+$ [5,10]. In our previous article [5], we focused on the case where the total amount of NADPH and $NADP^+$ remains constant and first considered that the second substrate, isocitrate, was in excess in the experiments. In a second stage, we allowed the isocitrate level to decrease in the course of time; bistability then occurred as a long-lived transient phenomenon.

To introduce the possibility of sustained oscillations, we subsequently considered the case where isocitrate is injected at a constant rate into the system. In such semi-open conditions schematized in Fig. 1 without short-dashed arrows, we obtained preliminary evidence for oscillations but lost the possibility of bistable behavior [11]. Before examining in the next section the case of fully open conditions (schematized by the full Fig. 1 including short-dashed arrows), we wish to investigate in further detail the occurrence of sustained oscillations in the semi-open conditions defined above. This case is of particular interest as it corresponds to simpler experimental realization, and as it is readily amenable to an analytical approach. In the following, the role of the second substrate of diaphorase, O_2, is disregarded as it can be considered as remaining constant in the medium.

2.1. Kinetic equations

The dynamics of the system is governed by two coupled kinetic equations describing the time evolution of the isocitrate and NADPH concentrations:

$$\frac{dI}{dt} = v - f(Z-P,P,I)$$
$$\frac{dP}{dt} = f(Z-P,P,I) - g(P) \quad (1)$$

where I, P indicate the concentrations of isocitrate and NADPH; the rate functions f and g relate, respectively, to the IDH and DIA reactions (see below). Parameters are defined in Table 1 where their experimental values are indicated. The concentration of the substrate $NADP^+$ (S) is obtained from the conservation relation (2):

$$S = Z - P \quad (2)$$

where Z denotes the total, constant amount of $NADP^+$ + NADPH.

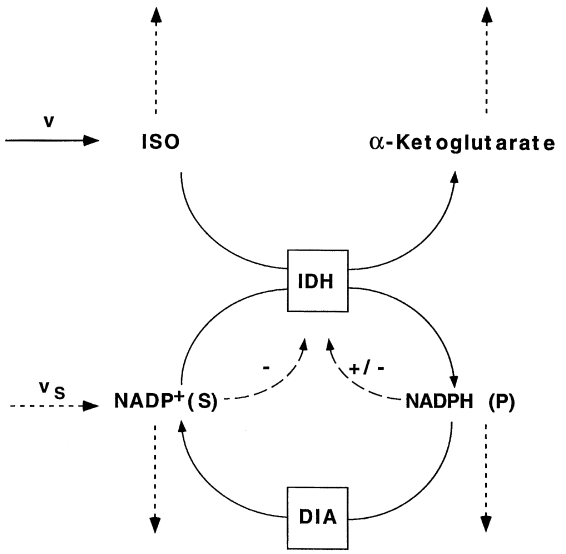

Fig. 1. The isocitrate dehydrogenase (IDH) reaction. The enzyme transforms tribasic isocitrate (ISO) and $NADP^+$ into α-ketoglutarate plus CO_2 and NADPH, respectively. Also indicated are the inhibition of IDH by $NADP^+$ as well as the inhibition and activation of this enzyme by NADPH. The reverse transformation of NADPH into $NADP^+$ is catalyzed by the enzyme diaphorase (DIA). The figure gives a schematic representation of the open IDH–DIA system with input of isocitrate (plain arrows) and with input of isocitrate and $NADP^+$ and efflux of all the metabolic species (plain and short-dashed arrows).

Table 1
Experimental values of the constants for the IDH rate [5–10]

k_0	$2\ s^{-1}$
k_1	$12.3\ s^{-1}$
K_m^I	17 μM
K_I	35 μM
K_A	0.25 μM
K_I'	7 μM
K_m^{III}	35 μM

The rate function $f(S,P,I)$ of IDH in system (1) is given by [5]:

$$f(S,P,I) = k_0 \frac{E_I S}{K_m^I(1+P/K_I)+S} \times \left(\frac{I}{K_m^{III}+I}\right) \times \left[1+\frac{k_1}{k_0}\frac{P}{K_A(1+S/K'_I)+P}\right] \quad (3)$$

where E_I denotes the concentration of IDH.

In this expression, the first term in the product accounts for the kinetic properties of the enzyme working with a minimum turnover number, k_0, and includes the competitive inhibition of IDH by its product NADPH (P) with an inhibition constant K_I. The term between brackets describes the change in turnover number due to the activation by NADPH with an activation constant K_A, which leads to the maximum turnover number $k_{\max} = k_0 + k_1$. This term also includes the inhibition by the substrate, $NADP^+$ (S), characterized by the inhibition constant K'_I.

Diaphorase can be regarded as a Michaelian enzyme, showing a high affinity for its substrate NADPH. The kinetic expression describing the transformation of NADPH into $NADP^+$ by diaphorase is thus given by the function $g(P)$:

$$g(P) = \frac{k_{\text{cat}} E_{II} P}{K_m^{II}+P} \quad (4)$$

where $k_{\text{cat}} = 0.8\ \text{s}^{-1}$ and E_{II} indicates the diaphorase concentration while K_m^{II} denotes the Michaelis–Menten constant of the enzyme [5,8,10]. Experimentally, the value of K_m^{II} was not determined precisely, but was found to be less than 1 μM. In the following we have chosen $K_m^{II} = 0.01$ μM.

The system of Eq. (1) admits a single steady state, because of the assumption of a constant input of substrate I:

$$P_0 = \frac{v_e K_m^{II}}{k_{\text{cat}} - v_e}$$

$$I_0 = \frac{v K_m^{III}}{f_1(Z-P_0,P_0) - v} \quad (5)$$

where $v_e = v/E_{II}$ and f_1 is given by Eq. (6):

$$f_1(S,P) = k_0 \frac{E_I S}{K_m^I(1+P/K_I)+S} \times \left(1+\frac{k_1}{k_0}\frac{P}{K_A(1+S/K'_I)+P}\right) \quad (6)$$

The conditions for the existence of a physically acceptable steady-state solution are found by imposing that P_0 and I_0 be positive and, according to Eq. (2), that P_0 be smaller than Z:

$$v_e < \frac{Z}{K_m^{II}+Z} k_{\text{cat}} \quad (7)$$

and

$$v_e < f_1(Z-P_0,P_0) \quad (8)$$

i.e.

$$e > v_e \frac{K_m^I(1+P_0/K_I)+Z-P_0}{(Z-P_0)(k_0+k_1P_0/(K_A(1+(Z-P_0)/K'_I)+P_0))} \quad (9)$$

where $e = E_I/E_{II}$.

2.2. Stability analysis and domain of sustained oscillations

Linear stability analysis of Eq. (1) leads to a second-degree characteristic equation which in turn yields the conditions in which sustained oscillations of the limit cycle type occur around an unstable steady state. Using this condition, it is possible to determine in parameter space the domain in which sustained oscillations of the limit cycle type occur. In the present situation, we have three main control parameters which are most readily amenable to experimental manipulation: these are parameter e which measures the ratio of IDH to DIA concentrations, parameter v_e which measures the input rate of isocitrate di-

vided by DIA concentration, and Z which is the total amount of $NADP^+ + NADPH$. Shown in Fig. 2 are the stability diagrams established as a function of these control parameters taken two by two at a time, together with the regions of existence of the steady state. Thus, in Fig. 2a, the domain of sustained oscillations is indicated as a function of e and v_e, for a given value of Z. The oscillatory domain is determined in Fig. 2b as a function of Z and v_e, for a given value of e, and in Fig. 2c as a function of Z and e, for a given value of v_e. The diagrams show that for each of the three control parameters there exists an oscillatory domain bounded by two critical values of the parameter. Moreover, the oscillatory domain progressively shrinks as parameters e and Z increase, whereas the size of the domain first increases, then passes through a maximum and later decreases as the value of parameter v_e rises. The diagrams of Fig. 2 also show the existence of a domain of stable steady-states and a domain in which the substrate I accumulates as the rate of isocitrate injection exceeds the maximum rate of IDH and/or DIA (this situation corresponds to the case when no physically acceptable steady state is found, below the dashed line, or when the system is not bounded, between the dotted and dashed lines).

The reason why the oscillatory domain shrinks as Z increases can be related to the mechanism of oscillations which primarily rests on the activation of IDH by its product NADPH (see below). As Z rises, so does the steady-state level of the substrate S since the steady-state level of product P does not change when Z varies; see Eqs. (2) and (5). As shown by Eq. (3), the effective value of the constant K_A which measures the activation of IDH by its product increases with the value of S, as a result of the inhibition of the enzyme by its substrate $NADP^+$. The larger Z, the larger the steady-state value of S, and thus the larger the value of the effective K_A, which corresponds to a decrease in autocatalysis. When the effective K_A increases beyond a critical value oscillations disappear altogether (see Fig. 3a) as the primary mechanism driving the instability becomes too weak to destabilize the steady state. Further

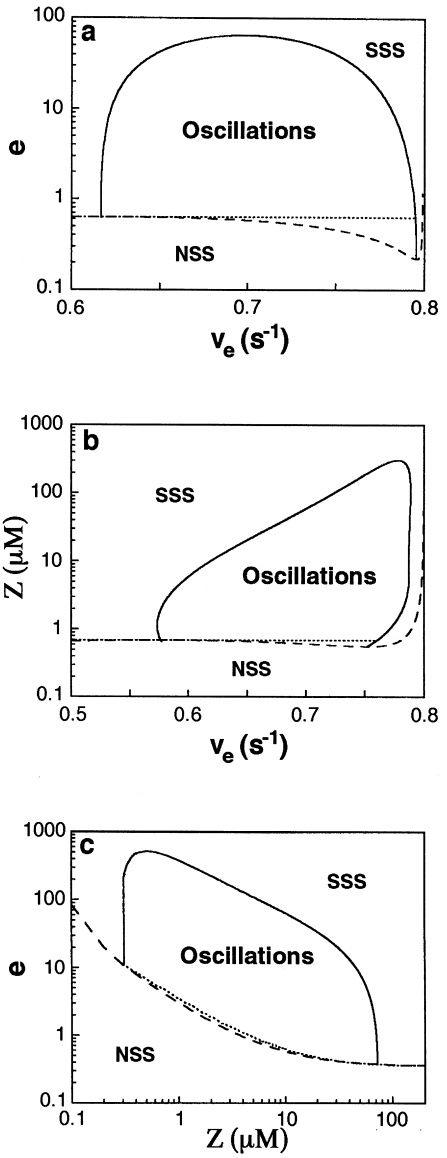

Fig. 2. Domains of sustained oscillations for system (1) as a function of parameters $e - v_e$ (a), $Z - v_e$ (b) and $e - Z$ (c). The system displays sustained oscillations in the regions bounded by the solid lines and the dotted lines, where the steady state given by Eq. (5) is unstable. The region marked SSS denotes a stable steady state. Below the dashed lines the system does not possess any steady state (region marked NSS) because relation (9) is not satisfied. In the latter situation, as well as in the case where the system possesses an unstable steady state and the phase space is not bounded (below the dotted line), model (1) predicts an accumulation of isocitrate. Parameter values are: $Z = 10$ μM (a), $e = 5$ (b) and $v_e = 0.7$ s^{-1} (c).

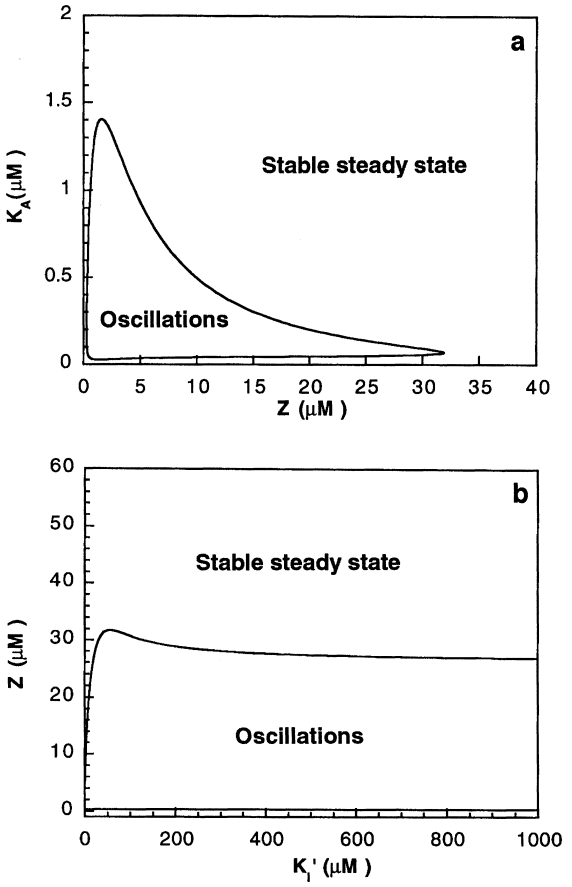

Fig. 3. Stability diagrams established as a function of parameter K_A, which measures the activation of IDH by its product NADPH, and Z (*a*), and as a function of Z and of parameter K'_I which measures the inhibition of IDH by its substrate $NADP^+$ (*b*). The domains of sustained oscillations are bounded by the loci of Hopf bifurcations, indicated by solid lines. As a function of K'_I, this domain extends to infinity (panel *b*), indicating that the primary cause of instability in system (1) is the activation of IDH by its product NADPH rather than substrate inhibition. In contrast, the domain is bounded by two critical values of K_A in panel *a*. Indeed, when K_A is too low, the enzyme is always activated and displays Michaelian behavior, whereas when K_A is too high the enzyme cannot activate in an efficient manner to generate sustained oscillations. The bifurcation loci have been determined numerically by means of the program AUTO [12]. Parameter values are: $e = 40$, $v_e = 0.7\ s^{-1}$.

weakening of autocatalysis as Z increases stems from the fact that IDH activity, which rises with the level of substrate S, reaches a larger and larger value even in the absence of enzyme activation by product P, as Z and S (but not P) increase.

That autocatalysis is the primary cause of instability rather than substrate inhibition is shown by the fact that the occurrence of sustained oscillations is not affected when this inhibition becomes negligible, at high values of parameter K'_I (see Fig. 3b which shows the stability diagram established as a function of parameters Z and K'_I).

2.3. Phase plane analysis and mechanism of limit cycle oscillations

Because the system contains only two variables, it is possible to resort to phase plane analysis to get a fuller picture of how oscillations arise in the coupled IDH–DIA enzymatic reactions. The two nullclines obey the following equations:

$$\frac{dP}{dt} = 0, \quad \text{or } I = \frac{K_m^{III} g(P)}{f_1(Z-P,P) - g(P)}$$

$$\frac{dI}{dt} = 0, \quad \text{or } I = \frac{K_m^{III} v}{f_1(Z-P,P) - v} \tag{10}$$

Of crucial importance for oscillations is the N shape of the product nullcline $dP/dt = 0$ (see inset to Fig. 4a where the product nullcline with its right limb is shown, together with the limit cycle) — this shape becomes that of a S-shaped sigmoid when P is plotted as a function of I. The steady state (black dot) lies at the intersection of this nullcline with that of the substrate isocitrate, $dI/dt = 0$. The latter nullcline moves toward the right when the input rate v_e of isocitrate increases. The product nullcline remains unchanged when this parameter varies, since v_e does not enter the equation of the P nullcline.

As in other instances of chemical or biochemical oscillations — see, e.g. the phase plane analysis of a model for glycolytic oscillations arising from the product-activated phosphofructokinase reaction [1] — the domain of instability corresponds to the region of sufficiently negative slope at steady state on the product nullcline. We show

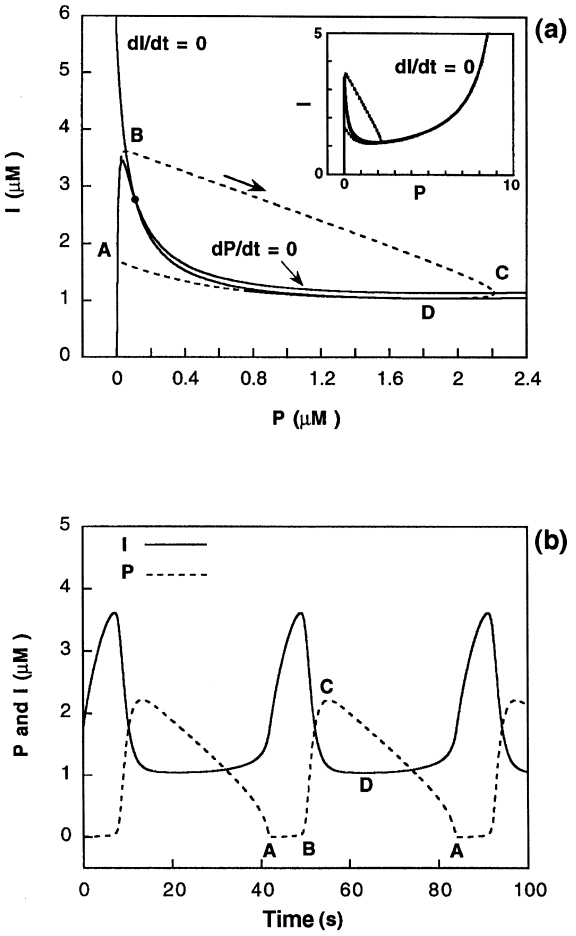

Fig. 4. Phase plane portrait (panel *a*) in a situation where an unstable steady state (black dot) is surrounded by a stable limit cycle (dashed line). The corresponding sustained oscillations are shown in panel *b*. Also shown in (*a*) are the P and I nullclines given by Eq. (10). Capital letters in panels *a* and *b* refer to the different phases of the oscillations (see text). The inset in panel *a* shows a broader view of the phase portrait, revealing the *N*-shape of the P nullcline. Parameter values are: $e = 7$, $\nu_e = 0.733\ s^{-1}$, $Z = 10$ μM. Here, as in the following figures unless differently indicated, the value of DIA concentration, E_{II}, is taken as 1 μM.

in Appendix A that the condition of instability here takes the form:

$$\left(\frac{dI}{dP}\right)_{(P_0,I_0)} < -1 \qquad (11)$$

on the P nullcline.

As parameter ν_e increases from a low initial value, the steady state is at first located on the left limb of the P nullcline, in a region of positive slope on this nullcline. Then, as ν_e further increases, the steady state moves into a region where this slope becomes negative: any increase in ν_e leads to an increase in P_0 accompanied by a decrease in the steady-state level of isocitrate, I_0. This happens as soon as autocatalysis by the product becomes sufficiently strong. Then, indeed, any increase in product due to the rise in ν_e will lead to stronger activation of IDH and, consequently, to an increase in consumption of the substrate I.

Sustained oscillations generated by the model are shown in Fig. 4b. In the case considered, the period is of the order of 40 s. The succession of events in the course of one period can be described as follows, if we divide the limit cycle shown in four parts (separated by points A, B, C and D in Fig. 4a,b). Starting at the minimum product concentration (point A), we observe that IDH is predominantly in its less active state characterized by the basal rate constant k_0, since product activation of the enzyme is at its minimum. Then the rate of isocitrate input exceeds the rate at which this substrate is transformed by IDH, so that isocitrate accumulates. This phase, the duration of which is primarily controlled by the value of ν_e, corresponds to the part AB of the limit cycle in Fig. 4a. During this phase the product P slowly accumulates until it reaches near B the threshold level at which it begins to activate IDH in an autocatalytic manner: a pulse of product synthesis ensues (part BC of the limit cycle).

Along BC, isocitrate (I) is consumed at a rate larger than the rate ν_e at which it is supplied, and the level of the second substrate, S, also drops since the sum of P (which increases) and S has to remain constant according to the conservation relation (2). Because of this drop in I and S, the rate of IDH will begin to decrease, until it becomes smaller than the rate of the second enzyme reaction, catalyzed by DIA, the rate of which has increased as a result of the rise in its substrate P, the product of IDH (given the low value of its Michaelis constant, DIA generally operates at a

nearly maximum rate). As soon as this happens, in C, the level of P begins to decrease. In D, the rate at which I is consumed in the IDH reaction drops below the value of v_e, so that isocitrate resumes its accumulation. Between D and A, the product NADPH is transformed by DIA into the substrate $NADP^+$, and P pursues its decline while S rises. This lasts until the rate of DIA declines (because of the drop in P which reaches very low levels) down to the value of the basal rate of IDH. Then P can again slowly increase as the system travels along the part AB of the limit cycle (see above). The parameter that drives this repetitive movement is the isocitrate influx, v_e.

The above described sequence of events along one cycle much resembles the repetetive activation–inactivation cycle observed for phosphofructokinase in the course of glycolytic oscillations [1]. One important difference, however, originates from the cyclical structure of the IDH–DIA bienzymatic system: a rise in the IDH reaction due to the rise in P inevitably leads both to a drop in the rate of this enzyme (as the level of substrate S decreases) and to an increase in the rate of the reverse reaction catalyzed by DIA. Therefore a rise in P can only lead to a subsequent decrease in product concentration.

The time evolution of I and P corresponding to these successive phases of the limit cycle is shown in Fig. 4b. It is interesting to determine how the sequential phases of the limit cycle and the very waveform of the oscillations are affected by a variation in the control parameters. As shown in Fig. 5a,b (in which $v_e = 0.633\ s^{-1}$ and $0.783\ s^{-1}$, respectively), to be compared with Fig. 4b (where $v_e = 0.733\ s^{-1}$), the duration of the phase AB decreases, while the duration of the phases CDA rises and the overall period increases from approximately 30 to 200 s as the value of v_e rises. The fact that the duration of AB shortens is simply due to the faster accumulation of substrate I, and thus of product P up to the activation threshold. The prolonged decrease of P along the path CDA results from the fact that as v_e rises, the rate of IDH remains closer to that of DIA so that the drop in P slows down.

Another factor that markedly influences the waveform and the period of the oscillations is the

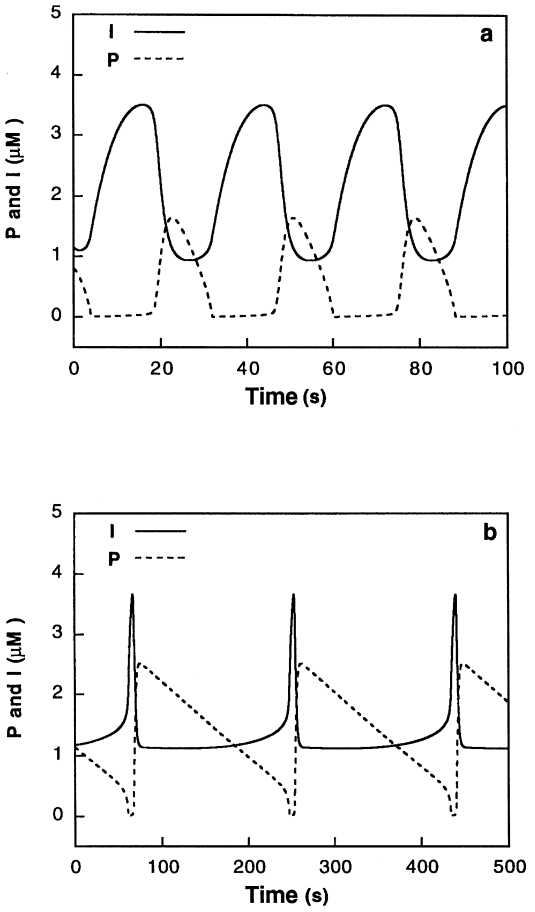

Fig. 5. Sustained oscillations for two different values of v_e ($0.633\ s^{-1}$ in *a*; $0.783\ s^{-1}$ in *b*). The two time series, to be compared with the time series of Fig. 4b (established for $v_e = 0.733\ s^{-1}$), show how the period and the waveform of the oscillations change as v_e increases (see text). Other parameter values are as in Fig. 4b.

ratio of IDH to DIA concentrations, denoted e. When this parameter decreases, the oscillations acquire a more pronounced relaxation nature (see Fig. 6 established for $e = 1$ to be compared with the value $e = 7$ in Figs. 4 and 5): the phases AB, BC and DA become very brief, while CD is by far the slowest phase. The latter phase, which corresponds to a long plateau in P, occupies the largest fraction of the period which itself increases significantly, up to approximately 1 h as compared to the oscillations seen in the model at larger values of e (see Figs. 4 and 5). The small spike on top of

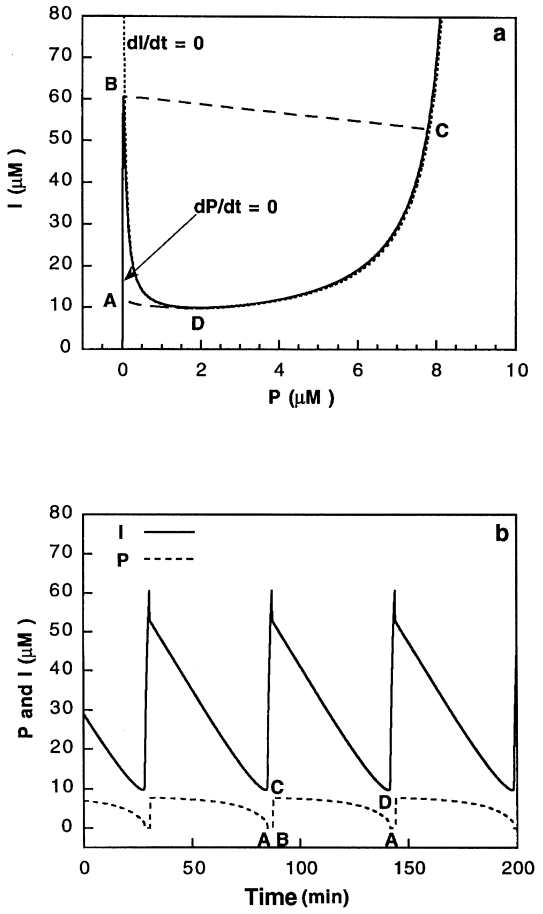

Fig. 6. Relaxation oscillations. (*a*) Phase plane portrait showing the P nullcline (solid line) and the I nullcline (dotted line) as well as the limit cycle (dashed line); (*b*) the corresponding sustained oscillations. As in Fig. 4, capital letters in panels *a* and *b* refer to the different phases of the oscillations. The situation, represented for $e = 1$, has to be compared with those in Figs. 4 and 5, established for higher values of e. When the latter parameter decreases, the oscillations acquire a more pronounced relaxation nature, and the period greatly increases (note that in panel *b*, time is measured in minutes). The values of v_e and Z are as in Fig. 5b.

the oscillations of I results from the fact that the rapid increase on AB is followed by a rapid move (along BC) to the right limb of the nullcline; this quasi-horizontal movement in the phase plane is accompanied by a slight decrease in I, and is followed by a much slower decline in I as the system moves along the path CD on the product nullcline. The jump from D to A also occurs rapidly and signals the end of the plateau phase. A comparison between Figs. 5 and 6 shows that a further reason why the relaxation nature of the trajectories is enhanced when e is smaller is that the left limb of the product nullcline goes up much more than at larger values of e.

2.4. Bifurcation diagrams for oscillatory behavior

The bifurcation diagrams of Fig. 7a,b established by means of the program AUTO [12] as a function of the isocitrate input rate v_e, show the steady-state levels (stable or unstable) of isocitrate (I) and NADPH (P), respectively, as well as the maximum and minimum of these variables in the course of sustained oscillations. These diagrams should prove useful in guiding experimental studies of the IDH–DIA bienzymatic system. The NADPH concentration P_0 remains low until the isocitrate input rate v_e reaches a value slightly smaller than 0.8 s^{-1}, that is the maximum rate of the enzyme diaphorase. Beyond this value of v_e, the NADPH steady-state concentration undergoes a steep increase. The main reason for this steep rise is that NADPH cannot be totally transformed back to $NADP^+$ because DIA approaches its maximum rate. The product concentration thus accumulates until it reaches its maximum value Z. Isocitrate steady-state concentration I_0 depends on P_0, which controls the activation of IDH, and the amount of its substrate S_0 in the medium, through the conservation relation (2). After a first rise (not shown in Fig. 7a), I_0 begins to decrease because of the progressive activation of IDH. When the enzyme is fully activated, a further increase in v_e leads to a rise in I_0.

Oscillations originate from the activation of IDH by its product NADPH (P). The amplitude of I remains practically independent from v_e (Fig. 7a) since it is dictated by the positions of points B and D on the product nullcline which does not depend on v_e (see Fig. 4). In contrast, the amplitude of P increases with v_e (Fig. 7b). The point C at which the product begins to decline must correspond to a larger value of P when v_e rises, since the rate of IDH, which rises with the level of its substrate I, has to be equal to the rate of DIA, which is close to its maximum value. The

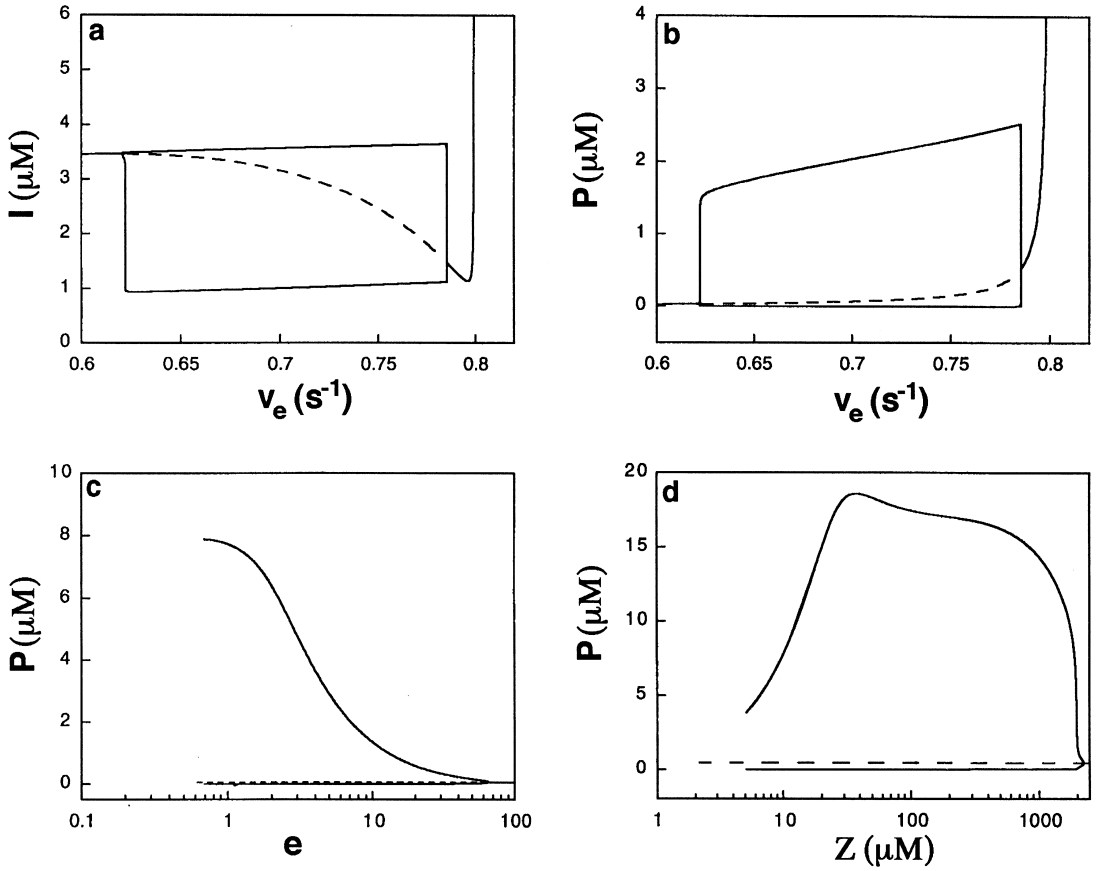

Fig. 7. Bifurcation diagrams for system (1). The isocitrate (I) and NADPH (P) steady-state concentrations, stable (solid line) or unstable (dashed line), are shown, together with the maximum and the minimum of their oscillations, as a function of parameter v_e, in panels *a* and *b*, respectively. The bifurcation diagram is shown for NADPH in panels *c* and *d* as a function of parameters *e* and *Z*, respectively. Whereas the region of oscillations is enclosed between two Hopf bifurcation points in panels *a* and *b*, in *c* and *d* it ends at low values of the control parameters because system (1) becomes unbounded and isocitrate accumulates in the medium (see text). Parameters are: $e = 7$ and $Z = 10$ μM in panels *a* and *b*; $Z = 10$ μM and $v_e = 0.7\ s^{-1}$ in panel *c*; $e = 1$ and $v_e = 0.783\ s^{-1}$ in panel *d*. The diagrams have been obtained as indicated in Fig. 3.

only way this may occur is by a decrease in the second substrate of IDH, $NADP^+$ (S). According to the conservation relation (2), such a decrease in S must be accompanied by a rise in P.

The diagrams of Fig. 7a,b have been obtained for the intermediate value $e = 7$. At higher values of e, e.g. $e = 50$, the envelope of the oscillations passes through a maximum and the decline in amplitude at the two extremities of the oscillatory domain is more gradual (not shown). Enlargements of the bifurcation diagrams of Fig. 7a,b show the existence of barely detectable small-amplitude limit cycles (stable or unstable) at the two extremities of the oscillatory domain (Fig. 8). The consequent abrupt change in the amplitude of the limit cycle as a function of v_e is associated with the existence in these regions of 'ducks' [13,14] (the name of the phenomenon alludes to the peculiar form of the limit cycle found in certain systems in similar conditions), or hard excitation (when the bifurcation is subcritical).

The bifurcation diagrams established for the amplitude of the product oscillations as a function of the other two control parameters, *e* and

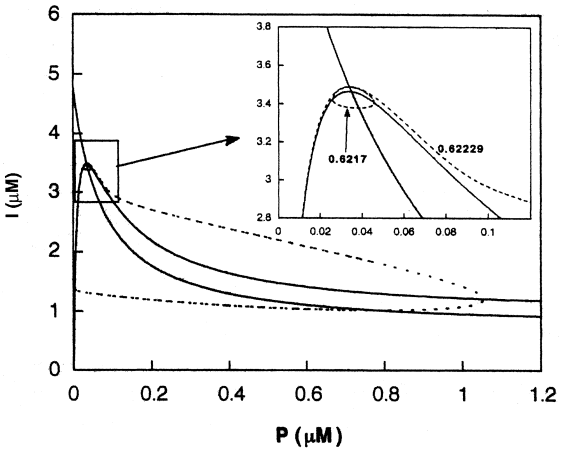

Fig. 8. Abrupt change in the amplitude of the limit cycle near the Hopf bifurcation point. The inset shows the small limit cycle obtained for $v_e = 0.6217\ s^{-1}$ and part of the large-amplitude cycle (shown entirely in the main figure) obtained for the close value $v_e = 0.62229\ s^{-1}$. In the inset, the two I-nullclines corresponding to the two v_e values are indistinguishable from each other. The P-nullcline, independent of v_e, is also represented. The abrupt variation in limit cycle amplitude is associated with the existence of a phenomenon known as 'duck' [13,14]. Parameter values are $e = 7$, $Z = 10$ μM.

Z, are shown in Fig. 7c,d, respectively. We observe that oscillations disappear for low values of e and Z when the system (1) looses its steady state or becomes unbounded.

How the period of the oscillations, T, varies with each of the control parameters is shown in Fig. 9. The dependence of T on v_e is shown for three distinct values of Z in Fig. 9a, and for three distinct values of e in Fig. 9b. In Fig. 9c,d is shown the variation of T as a function of e and Z. The period generally ranges from some 30 s to 10 min or so, but can reach values outside this range near the extremities of the oscillatory domain in parameter space (see, for example Fig. 6 established for $e = 1$). After a steep rise, the period increases by about one order of magnitude as v_e rises (panels a and b), and increases even more as parameters e and Z decrease (see Figs. 4 and 6). This occurs because the nullcline $dP/dt = 0$ has a local maximum which is pushed upward as e and Z decrease. As a result, it takes more and more time for the system to travel on the AB part of the limit cycle — this causes the period to increase.

3. Model for the IDH reaction with input of isocitrate and NADP$^+$ and efflux of all metabolic species

So far we have analyzed the model for the IDH–DIA bienzymatic system in conditions permitting either bistability or oscillations. Thus, in our first publication devoted to the analysis of this model in the absence of any influx of substrate, we recovered the phenomenon of transient bistability observed in the experiments performed in closed conditions [5]. In a subsequent publication [11] and in the first part of this work, we showed that oscillations — but not bistability — can occur when the system becomes open to an influx of isocitrate. The question arises as to whether bistability and oscillations can both occur in the same type of experimental conditions in the IDH–DIA cyclical reaction system. In this section we show that this possibility indeed exists if the system operates as an open reactor with an influx of the substrates isocitrate and NADP$^+$, and an efflux of all metabolic species (see Fig. 1, with both solid and dashed lines).

3.1. Kinetic equations

The kinetic equations of the model in these fully open conditions take the form of Eq. (12):

$$\frac{dS}{dt} = v_S - f(S,P,I) + g(P) - kS$$

$$\frac{dP}{dt} = f(S,P,I) - g(P) - kP$$

$$\frac{dI}{dt} = v - f(S,P,I) - kI \qquad (12)$$

where $f(S,P,I)$ and $g(P)$ denote, as before, the rate function of IDH and DIA [see Eqs. (3) and (4)]; moreover, k is the constant flow rate through the reactor, defined as the volume fraction that both enters and leaves the reactor per unit time, and v_S is the constant inflow of NADP$^+$. The inflow rates of NADP$^+$ and isocitrate, v_S and v,

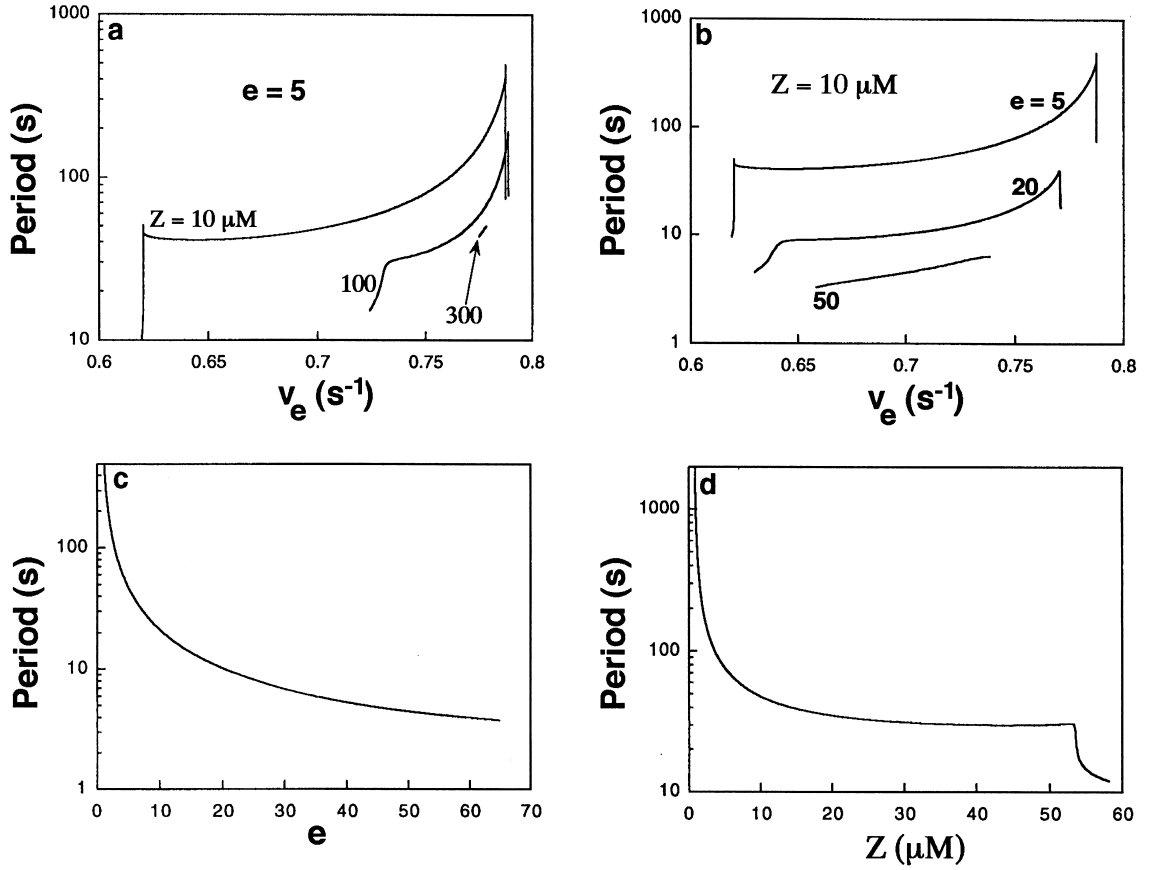

Fig. 9. Dependence of the period of oscillations on the main control parameters. The variation of the period as a function of v_e is shown in panels *a* and *b* for three distinct values of Z and e, respectively, whereas only one pair of values of Z and v_e ($Z = 10$ μM, $v_e = 0.7\ s^{-1}$) and of e and v_e ($e = 5$, $v_e = 0.7\ s^{-1}$) is considered in panels *c* and *d*. The increase of the period at low values of e and Z in panels *c* and *d* is related to the approach of the domain of isocitrate accumulation (see text).

can be expressed as the product of the constant flow rate k by their concentrations S_{in} and I_{in} in the input streams.

We can reduce the three differential equations [Eq. (12)] to a system of two differential equations, considering that the total concentration of $NADP^+ + NADPH$, $Z = S + P$, will evolve towards a constant value determined by the ratio of v_S and k. Indeed, adding the first two equations of system (12), we find the evolution equation for Z :

$$\frac{dZ}{dt} = v_S - kZ \tag{13}$$

According to this equation, Z will evolve, with a characteristic time of $1/k$, towards the value $Z = v_S/k = S_{in}$. Thus we can assume that, after a certain time, the dynamics of the system will be described by two differential equations for P and I, plus an algebraic relation involving the concentrations of S and P:

$$\frac{dP}{dt} = f(S,P,I) - g(P) - kP$$

$$\frac{dI}{dt} = kI_{in} - f(S,P,I) - kI$$

$$S + P = S_{in} \tag{14}$$

The steady states are found solving the algebraic equations:

$$I_0 = \frac{v - g(P_0) - kP_0}{k}$$

$$v - f(S_{in} - P_0, P_0, I_0) - kI_0 = 0 \qquad (15)$$

Introducing the first into the second of these equations, we obtain an equation of the sixth degree in P_0 that can be solved numerically. The presence of k ensures the existence of at least one steady state as the outflow prevents the accumulation of isocitrate. This is an important difference between system (14) and the system without outflow that we have analyzed in the previous sections. Moreover, Eq. (15) do not ensure anymore the uniqueness of a positive steady state and can have up to three acceptable solutions. Due to the outflow, the system can thus display bistability, as will be seen below.

3.2. Domain of sustained oscillations and bistability

Here we have four main control parameters which are most readily amenable to experimental manipulation: these are e, S_{in}, I_{in}, and parameter $k_e = k/E_{II}$ which measures the ratio of the constant flow rate through the reactor, divided by DIA concentration. Shown in Fig. 10 are the stability diagrams established as a function of S_{in} and e vs. k_e. The domain of oscillations, within the dashed lines, is bounded between two critical values of k_e.

In both diagrams, we observe a domain of bistability (enclosed by solid lines) for values of parameter k_e larger than the upper critical value for the domain of oscillations. The region of bistability is also bounded between two critical values of k_e and overlaps with the domain of oscillations, thus giving rise to situations where the limit cycles enclose three unstable steady states.

By a comparison of the diagrams of Fig. 10 with those of Fig. 2 established for the system without outflow, we notice that the main differences arise in the region where system (1) does not possess any physically acceptable steady state and isocitrate accumulates in the medium. It is precisely in this region that bistability appears in fully open system (12). In contrast, the domain of sustained oscillations remains substantially unchanged (compare Fig. 2b and Fig. 10b). The critical values

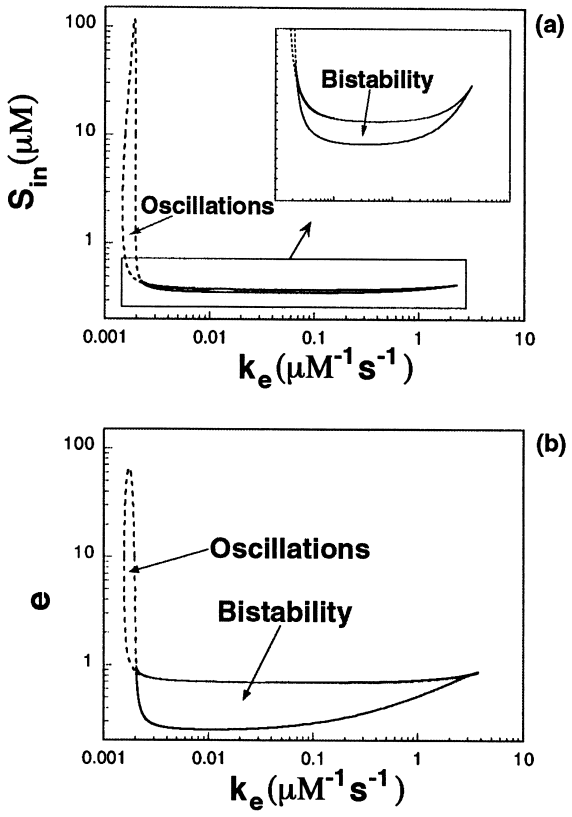

Fig. 10. Two-parameter bifurcation diagrams for the open system (12) established as a function of parameters $S_{in} - k_e$ (*a*), and $e - k_e$ (*b*). The loci of limit points bounding the domain of bistability are represented by solid lines; the loci of Hopf bifurcations bounding the domain of sustained oscillations are represented by dashed lines. Outside these regions the system displays monostability. The domains of bistability have the shape of a crescent (see the enlargement in panel *a*), which makes it possible to observe mushrooms and isolas as a function of parameter k_e (see Fig. 12). When the two domains overlap the system can have three steady states surrounded by a stable limit cycle; however, the system cannot show sequentially bistability and sustained oscillations as a function of only one of the parameters considered in the diagrams. Parameter values are: $I_{in} = 400$ μM and $e = 10$ in panel *a*; $I_{in} = 400$ μM and $S_{in} = 10$ μM in panel *b*. The bifurcation boundaries are obtained as in Fig. 3.

which bound this domain are nearly the same for the two models, as can be seen when recalling the relation $v_e = k_e\ I_{in}$ between the input rate of isocitrate, v_e, and its input concentration, I_{in}. Due to the low value of k_e in the oscillatory domain, the outflow does not affect significantly the dynamics of system (12); thus the two models display the same behavior. The oscillations have the same appearance as in Figs. 4–6. Moreover, the effect of the flow rate k_e on the period is similar to that of parameter v_e in system (1) (see Fig. 9).

3.3. Phase plane analysis and bistability

We have just seen that the domain of oscillations extends at small values of parameter k_e, for which the role of the outflow in the dynamics of system (12) can be considered as unimportant. The mechanism and the main characteristics of oscillations remain substantially the same as in the model without outflow. However, as system (12) always possesses a steady state, for low values of e and S_{in} (that here plays the role of Z), we observe as a function of these two parameters a second Hopf bifurcation that marks the vanishing of the oscillations (Fig. 10a,b), while in system (1) the oscillations stopped at low values of these parameters (see Fig. 2a,b and Fig. 7c,d) not as a result of a Hopf bifurcation but because of the accumulation of isocitrate in the medium. As a consequence, the rise in period seen when system (1) approaches the domain of substrate accumulation (see Fig. 6) is not observed for system (12) which operates in fully open conditions.

Also in contrast to the behavior of system (1), bistability appears in system (12) because of the presence of the outflow, when the product of k_e times I_{in} (i.e. v_e) exceeds a value around 0.8 s^{-1}. The origin of bistability can easily be understood by resorting to phase plane analysis. The nullclines for system (12) obey the following equations:

$$\frac{dP}{dt} = 0, \quad \text{or}$$

$$I = \frac{K_m^{III}(g(P) + kP)}{f_1(S_{in} - P, P) - g(P) - kP}$$

$$\frac{dI}{dt} = 0, \quad \text{or} \quad I = \frac{(kI_{in} - f_1(S_{in} - P, P) - kK_m^{III}) + \sqrt{(kI_{in} - f_1(S_{in} - P, P) - kK_m^{III})^2 + 4k^2 I_{in} K_m^{III}}}{2k} \tag{16}$$

Bistability corresponds to the existence of three intersections between the two nullclines of Eq. (16). In Fig. 11b these two nullclines are drawn for parameter values corresponding to a point inside the domain of bistability. For these parameter values, the P-nullcline given by Eq. (16) consists of two separated branches as for the P nullcline of the system without outflow, shown in Fig. 11a, but the shape of the I nullcline differs for the two models. One can show that for system (1) the latter nullcline cannot intersect with the P nullcline, in contrast to what is observed in presence of an outflow.

3.4. Different patterns of bistability

The bifurcation diagrams of Fig. 12 established as a function of the constant flow rate k_e show, for different values of parameter e, the steady-state levels (stable or unstable) of NADPH (P), as well as the maximum and minimum of this variable in the course of sustained oscillations. In panel a, obtained for a large value of e, monostability without oscillations is observed over the whole range of variations of k_e. The steady-state profile for NADPH (P) and I (not shown) is the same as for the model without outflow (see Fig. 7b). Oscillations arise for smaller values of e just before the steep increase of NADPH concentration (panel b), when the steady state becomes unstable as NADPH has reached a sufficient level to activate the enzyme IDH. These oscillations display the same characteristics as those in system (1), because in this region the outflow has only a minor effect on the dynamics of system (12).

When e enters the domain of bistability (panel c), we observe a bifurcation diagram of the sort referred to as 'mushroom' [15,16]. The passage from the low NADPH concentration to the high concentration steady state is accompanied by a

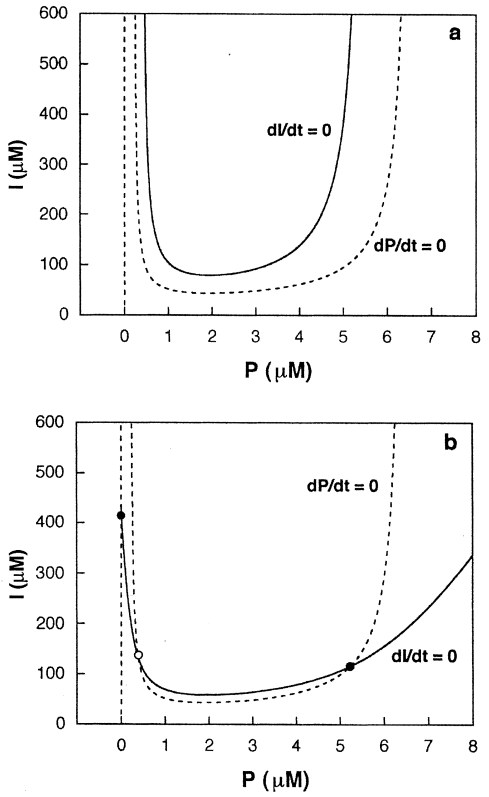

Fig. 11. Absence of bistability (*a*) in system (1) and presence of the phenomenon (*b*) in system (12). Shown in panel *b* is a phase portrait of system (12) in a situation of bistability. The three intersections between the *P* nullcline (dashed lines) and the *I* nullcline (solid line) correspond to three stationary states, two of which are stable (black dots) and one is unstable (empty circle). A comparison with panel *a* shows that bistability does not occur in system (1) because the *I* nullcline changes so that it cannot intersect with the *P* nullcline, a situation which results in isocitrate accumulation (see text). Parameter values are $e = 0.4$, $v_e = 1\ s^{-1}$, $Z = 10\ \mu M$ for panel *a*, and for panel *b*, $e = 0.4$, $k_e = 0.00167\ \mu M^{-1}\ s^{-1}$, $S_{in} = 10\ \mu M$, $I_{in} = 0.598$ mM.

phenomenon of bistability where the two stable steady states coexist and are separated by an unstable steady state. Two domains of hysteresis can be observed as a function of parameter k_e.

For lower values of e, the two hysteresis loops of panel *c* merge, giving rise to an isola (panel *d*) [15,16]. Isolas represent branches of multiple stable steady states which are not connected to each other through an unstable steady state. This particular configuration excludes the possibility to pass from one of the stable steady states to the other through an hysteresis mechanism. Thus we encounter here an example of irreversible transitions between two steady states [17,18]: upon changing k_e, the system can fall down from the high to the low concentration steady state, but cannot accomplish the reverse transition.

The origin of the mushroom and of the isola can be followed in the two-parameter bifurcation diagram of Fig. 10. The bistability domain has the shape of a crescent; its contour lines are the loci of the limit points associated with bistability. For $e = 0.8$, upon increasing k_e, we encounter four times the loci of limits points. Each intersection corresponds to a limit point in the bifurcation diagram of the system. The system thus passes from monostability to a zone of bistability bounded by the first two limit points. This zone is followed by a region of monostability and again by a zone of bistability bounded by the third and the fourth limit points. This is the situation in which the bifurcation diagram of Fig. 12c has the shape of a mushroom. Lowering e, the second and the third limit points approach and coalesce, giving rise to an isola (Fig. 12d for $e = 0.4$).

4. Discussion

The search for new oscillatory enzyme reactions is motivated by the fact that only a few examples of such reactions have been described so far. The best examples still are provided by the peroxidase reaction, glycolytic oscillations, and the periodic synthesis of cyclic AMP in the slime mold *Dictyostelium discoideum*. Oscillations of cytosolic Ca^{2+} have also been found in a large variety of cell types, but these oscillations do not originate from the regulation of enzyme reactions as in the other instances cited above. Moreover, there is a need for studying oscillations in well defined, minimal in vitro systems. If peroxidase fits this definition, glycolytic oscillations involve a large number of enzyme reactions and it is not easy to reconstitute a minimal glycolytic system capable of displaying sustained oscillatory behavior in vitro. Finally, the oscillatory synthesis of cyclic AMP can only be observed in intact *Dic-*

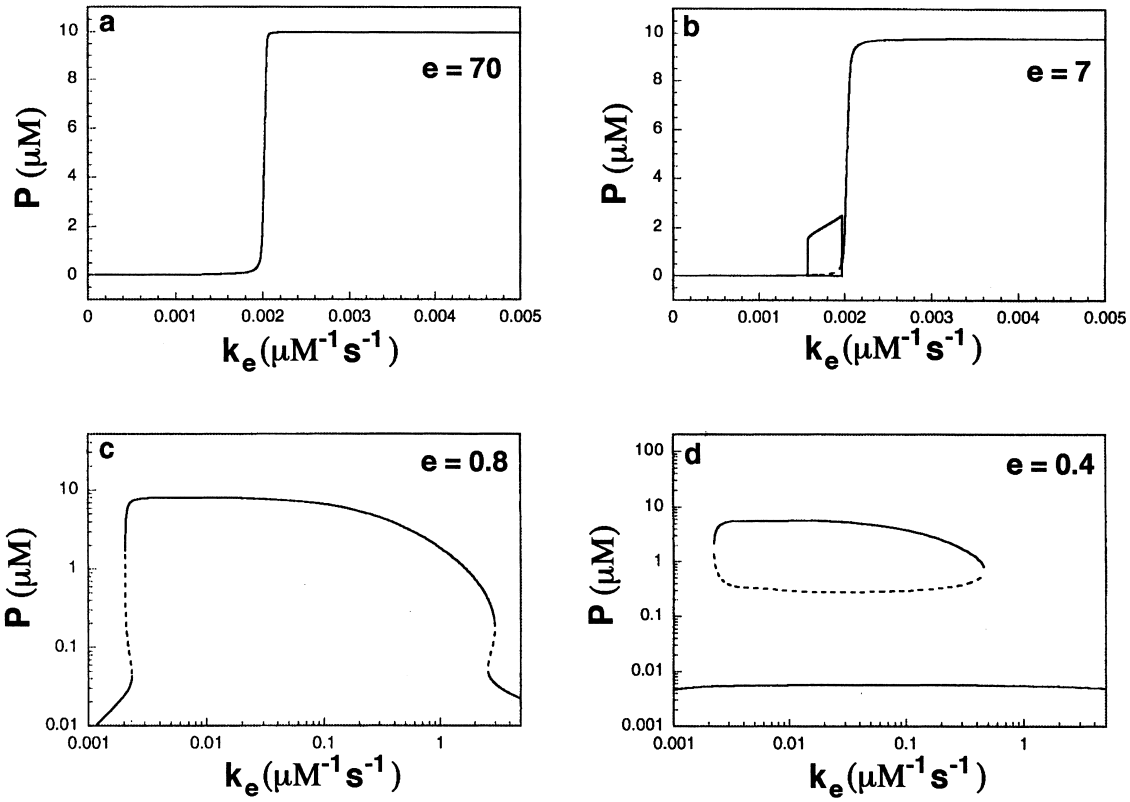

Fig. 12. Bifurcation diagrams for the open system (12) as a function of the flow rate k_e. The NADPH steady-state concentration, stable (solid line) or unstable (dashed line), is shown for decreasing values of e, indicated in each diagram. Also shown in panel b are the maximum and the minimum of the oscillations of NADPH. The system can display monostability (a); sustained oscillations (b); bistability with hysteresis in two different ranges of variation of parameter k_e, a situation which gives rise to a 'mushroom' (c); and bistability with an isola (d). In (b), the branch of the minima of oscillations is close to and thus masks the unstable steady state. Parameter values are as in Fig. 10.

tyostelium cells, and it has not been possible so far to reconstitute a minimal oscillating system in vitro, if only because the mechanism of oscillations relies on the activation of adenylate cyclase via the binding of cyclic AMP to its membrane receptor.

The bienzymatic system composed of isocitrate dehydrogenase (IDH) and diaphorase (DIA) is of a cyclical nature, given that each enzyme transforms the product into the substrate of the other enzyme (see Fig. 1). Here we have analyzed the conditions in which this bienzymatic system can give rise to sustained oscillations. Our previous analysis [5] had shown that the model proposed for the IDH–DIA coupled reactions can account for the experimental observations of Carlier [10], which pointed to the occurrence of bistability in this system. The present results indicate that this bienzymatic system is a good candidate for further theoretical and experimental studies of bistability and oscillations in a biochemical context.

We have studied the IDH–DIA system in three types of conditions. Our first approach [5] dealt with the system in closed (batch) conditions, when no substrate is provided and no volumic outflow occurs. Then, transient bistability can be observed over significant time intervals, as in the corresponding experiments. In the present work, we extended the analysis to the case where one of

the substrates, isocitrate, is supplied at a constant rate but no outflow occurs. In these conditions, oscillations can be observed with a period that generally ranges from 30 s to 10 min (smaller or larger periods can, however, be obtained at the extremities of the oscillatory domain in parameter space). As indicated in a preliminary study [11], bistability is ruled out in these conditions; moreover, the system sometimes displays substrate (isocitrate) accumulation in the course of time. Finally, we have shown in the present article that when the system is fully open to an influx of the two substrates of IDH and an efflux of all species, oscillations as well as bistability can occur. A steady state always exists in such conditions. Furthermore, different modes of bistability can be observed as the ratio of IDH to DIA concentrations (measured by parameter e) varies, namely, bistability with hysteresis, mushrooms, and isolas (see Fig. 12).

The present study therefore indicates that the study of the bienzymatic system in fully open conditions should provide the best opportunities to observe a rich variety of non-linear modes of dynamic behavior in this cyclical reaction system.

Can bistability and oscillations both be observed in the IDH–DIA system as a function of a single control parameter? Such a situation has not been found in our analysis. Therefore, to pass, for example, from bistability to oscillations, one should first decrease the value of parameter k_e and increase the value of either the concentration of the substrate $NADP^+$ in the input stream (S_{in}) or parameter e (see Fig. 10).

Many enzymatic systems are organized in a cyclical manner. Kinases and phosphatases (or enzymes catalyzing other types of covalent modification of proteins) provide important examples of such cyclical systems. The present results raise the question as to whether oscillations and bistability can arise in these other cyclical systems. Clearly, the regulatory properties of IDH, reflected by the highly non-linear nature of the phenomenological Eq. (3) describing the enzyme rate function plays a primary role in the origin of non-linear dynamic phenomena. Other studies of cyclical enzymatic systems [4,17], among which the self-activating calmodulin–kinase reaction coupled to the corresponding phosphatase [19], confirm that bistability, as well as oscillations [20,21], require the appropriate regulation by negative or positive feedback of at least one of the enzymes of the cyclical system.

Even if they might lack in direct physiological significance, since IDH and DIA do not appear to function in tandem in vivo, the present results indicate that isocitrate dehydrogenase, coupled to a second enzyme such as diaphorase (or another enzyme for that matter, since diaphorase is not regulated), may provide a useful model and a new example of enzyme reaction to be studied in vitro for a rich variety of non-linear modes of dynamic behavior, including oscillations and bistability.

Acknowledgements

This work was supported by the programme 'Actions de Recherche Concertée' (ARC 94-99/180) launched by the Division of Scientific Research, Ministry of Science and Education, French Community of Belgium.

Appendix A: Instability condition in the phase plane for system (1)

As the system is bidimensional, the stability of the steady state (P_0, I_0) is determined by the sign of the trace Tr of the Jacobian matrix. The positivity of Tr, given by Eq. (A1) evaluated at the steady state, ensures that the steady state is unstable:

$$Tr = \left(\frac{\partial \dot{P}}{\partial P} + \frac{\partial \dot{I}}{\partial I} \right)_{P_0, I_0} > 0 \qquad \text{(A1)}$$

i.e.:

$$\left(\frac{\partial \dot{P}}{\partial P} \right)_{P_0, I_0} > - \left(\frac{\partial \dot{I}}{\partial I} \right)_{P_0, I_0} = \left(\frac{\partial f}{\partial I} \right)_{P_0, I_0} > 0 \qquad \text{(A2)}$$

where f is the rate function of IDH [see Eq. (3)]; as the dependence of f on I is of a Michaelian type, its derivative is always positive.

As previously done in a model for glycolytic oscillations (see Goldbeter [1]), it is possible to relate this instability condition to the position of the steady state on the product nullcline $\mathrm{d}P/\mathrm{d}t = 0$. Indeed we can express the derivative $\mathrm{d}I/\mathrm{d}P$ of the product nullcline as:

$$\frac{\mathrm{d}I}{\mathrm{d}P} = -\frac{\partial\dot{P}/\partial P}{\partial\dot{P}/\partial I} \tag{A3}$$

The denominator of Eq. (A3) can be expressed in term of the derivative of f. We thus have, taking into account condition (A1):

$$\left(\frac{\mathrm{d}I}{\mathrm{d}P}\right)_{P_0,I_0} = -\left(\frac{\partial\dot{P}/\partial P}{\partial f/\partial I}\right)_{P_0,I_0} < -\left(\frac{\partial f/\partial I}{\partial f/\partial I}\right)_{P_0,I_0} = -1 \tag{A4}$$

which is the instability condition given in Eq. (11).

References

[1] A. Goldbetter, Biochemical Oscillations and Cellular Rhythms: The Molecular Bases of Periodic and Chaotic Behaviour, Cambridge University Press, Cambridge, UK, 1996.

[2] B. Hess, Q. Rev. Biophys. 30 (1997) 121.

[3] H. Degn, Nature 217 (1968) 1047.

[4] W. Schellenberger, J.F. Hervagault, Eur. J. Biochem. 195 (1991) 109.

[5] G.M. Guidi, M.F. Carlier, A. Goldbeter, Biophys. J. 74 (1998) 1229.

[6] M.F. Carlier, D. Pantaloni, Eur. J. Biochem. 37 (1973) 341.

[7] M.F. Carlier, D. Pantaloni, G. Branlant, J.F. Biellmann, FEBS Lett. 62 (1976) 236.

[8] M.F. Carlier, D. Pantaloni, Biochemistry 15 (1976) 1761.

[9] M.F. Carlier, D. Pantaloni, Biochimie 58 (1976) 27.

[10] M.F. Carlier, Thèse de Doctorat en Sciences. Univ. Paris-Sud, Paris, 1976.

[11] G.M. Guidi, A. Goldbeter, Biophys. Chem. 72 (1998) 201.

[12] E.J. Doedel, Congr. Num. 30 (1981) 265.

[13] W. Eckhaus, Lecture Notes on Mathematics 985, Springer-Verlag, Berlin, 1983, p. 432.

[14] S.M. Baer, T. Erneux, SIAM J. Appl. Math. 46 (1986) 721.

[15] N. Ganapathisubramanian, K. Showalter, J. Chem. Phys. 80 (1983) 4177.

[16] P. Gray, S.K. Scott, Chemical Oscillations and Bistability, Clarendon Press, Oxford, 1994.

[17] J.F. Hervagault, S. Canu, J. Theor. Biol. 127 (1987) 439.

[18] G.M. Guidi, A. Goldbeter, J. Phys. Chem. A. 101 (1997) 9367.

[19] J.E. Lisman, Proc. Natl. Acad. Sci. USA 82 (1985) 3055.

[20] J. Ricard, J.-M. Soulié, J. Theor. Biol. 95 (1982) 105.

[21] M.A. Coevoet, J.F. Hervagault, Biochem. Biophys. Res. Comm. 234 (1997) 162.